

References and Notes

1. A. E. Ringwood, *J. Geophys. Res.* **67**, 857 (1962); F. Birch, in *The Earth's Crust and Upper Mantle*, P. J. Hart, Ed. (American Geophysical Union, Washington, D.C., 1969), p. 18.
2. D. H. Green and A. E. Ringwood, *Contrib. Mineral. Petrology* **15**, 103 (1967); M. J. O'Hara, *Earth-Sci. Rev.* **4**, 69 (1968).
3. L. H. Cohen, K. Ito, G. C. Kennedy, *Amer. J. Sci.* **265**, 475 (1967).
4. K. Ito and G. C. Kennedy, *ibid.*, p. 519; I. Kushiro, Y. Syono, S. Akimoto, *J. Geophys. Res.* **73**, 6023 (1968).
5. A. L. Boettcher and P. J. Wyllie, *J. Geol.* **76**, 235 (1968).
6. I. B. Lambert and P. J. Wyllie, *Nature* **219**, 1240 (1968).
7. A. E. Ringwood, *Geochim. Cosmochim. Acta* **30**, 41 (1966).
8. B. E. Nordlie, *Geol. Soc. Amer. Spec. Pap.* **115**, 166 (1968).
9. W. W. Rubey, in *Crust of the Earth*, A. Poldervaart, Ed. (Geological Society of America, New York, 1955), p. 631; H. Holland, in *Petrologic Studies*, A. E. J. Engel, H. L. James, B. F. Leonard, Eds. (Geological Society of America, New York, 1962), p. 447.
10. Similar to the olivine tholeiite, 1921 flow of Kilauea, Hawaii, listed as No. 14, Table 2, by H. S. Yoder, Jr., and C. E. Tilley, *J. Petrol.* **3**, 342 (1962).
11. F. R. Boyd and J. L. England, *J. Geophys. Res.* **65**, 741 (1960).
12. A. Muan, *Amer. Ceram. Soc. Bull.* **42**, 344 (1963).
13. J. R. Holloway, C. Wayne Burnham, G. L. Millhollen, *J. Geophys. Res.* **73**, 6598 (1968).
14. R. E. T. Hill and A. L. Boettcher, in preparation.
15. A. L. Boettcher, *Trans. Amer. Geophys. Union* **50**, 352 (1969); H. S. Yoder, Jr., and I. Kushiro, *Amer. J. Sci.* **267-A**, 558 (1969).
16. S. P. Clark, Jr., and A. E. Ringwood, *Rev. Geophys.* **2**, 35 (1964).
17. H. J. Greenwood, *J. Geophys. Res.* **66**, 3923 (1961).
18. E. Roedder, *Amer. Mineral.* **50**, 1746 (1965).
19. A. L. Boettcher and P. J. Wyllie, *Amer. J. Sci.* **267**, 875 (1969); *Nature* **216**, 572 (1967).
20. P. J. Wyllie and O. F. Tuttle, *Amer. J. Sci.* **257**, 648 (1959).
21. C. Wayne Burnham, in *Geochemistry of Hydrothermal Ore Deposits*, H. L. Barnes, Ed. (Holt, Rinehart & Winston, New York, 1967), p. 34.
22. F. Press, *Science* **165**, 174 (1969).
23. H. Spetzler and D. L. Anderson, *J. Geophys. Res.* **73**, 6051 (1968).
24. J. R. Holloway, private communication.
25. We thank C. Wayne Burnham for helpful discussion and for reviewing the manuscript. R. Z. Small and Miss Tony Gardner assisted us in the laboratory. This work was supported by grant GA-1364 from the National Science Foundation.

21 November 1969; revised 15 December 1969 ■

Magnetic Particles Extracted from Manganese Nodules: Suggested Origin from Stony and Iron Meteorites

Abstract. *On the basis of x-ray diffraction and electron microprobe data, spherical and ellipsoidal particles extracted from manganese nodules were divided into three groups. Group I particles are believed to be derived from iron meteorites, and Group II particles from stony meteorites. Group III particles are believed to be volcanic in origin.*

Cosmic spherules in manganese nodules were first recognized by Murray and Renard (1), but no detailed study of their characteristics has been published. Since manganese nodules apparently grow more slowly than deep sea sediments are deposited (2), it ap-

peared possible to obtain significant numbers of spherules from relatively small amounts of material, unbiased by the addition of recent industrial contaminants.

Twenty-one manganese nodules and manganese oxide crusts from various oceanographic stations were crushed, and the magnetic fraction was removed with a hand magnet covered with cellophane. Fifty-five spherical and ellipsoidal particles were handpicked from the magnetic fractions under a binocular microscope.

The mean concentration of the magnetic spherules in manganese nodules is about 400 spherules ($>100 \mu\text{m}$ in diameter) per kilogram of sample and ranges from 0 to about 3500 per kilogram. This concentration is higher than the concentration of spherules in deep sea sediments ($330 > 30 \mu\text{m/kg}$) (3), salt deposits ($4 > 25 \mu\text{m/kg}$) (4), and beach sands ($6 > 180 \mu\text{m/kg}$) (5).

Nineteen spherules were analyzed by x-ray diffraction (powder and precession cameras) and electron microprobe techniques. The spherules were divided

into four categories (Table 1). Ten of the 19 spherules (Group I) are black, shiny, spherical, and commonly have a depression or dimple on the surface. Each spherule consists of an oxide phase of magnetite and wüstite, both containing 1 to 4 percent nickel, commonly surrounding an acentric, metallic nucleus containing about 50 to 75 percent nickel (Fig. 1). Precession photographs show that the magnetite, which usually forms an outer shell, is a homogeneous single crystal. The wüstite phase, visible in Fig. 1 as an inner shell, is probably a single crystal since it gives a spotty powder photograph, as does the magnetite; however, it was not positively identified in the precession photographs. The metallic core is polycrystalline.

The three Group II spherules are also black, shiny, and spherical, but without dimples. Precession photographs show that they consist of multicrystalline aggregates of magnetite and wüstite with nearly parallel orientations. In one particle (Albatross 13, No. 2), the oxide phase surrounds a nickel-rich metallic nucleus. The oxide phase of Group II particles is transected by a rectangular network of lamellas containing major iron and subordinate silicon and lesser amounts of magnesium, aluminum, and calcium (Fig. 2).

The internal structure and preferred crystallographic orientation of Group II spherules suggests that the oxide phase was formed by dendritic growth, and thus the silicate phase was confined to the interdendritic area. The absence of a diffraction pattern from the silicate phase may be due to its

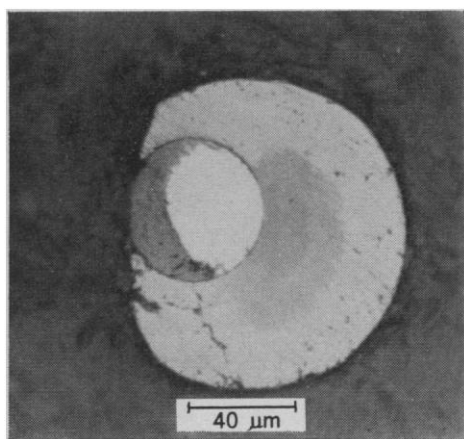


Fig. 1. Challenger 276, No. 1. This Group I particle shows a magnetite (light-gray) outer shell, wüstite (medium-gray) inner shell, and a metallic nucleus (white), which is partly oxidized to trevorite (dark gray).

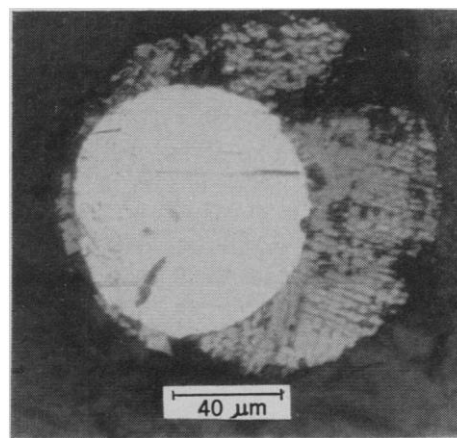


Fig. 2. Albatross 13, No. 2. This Group II particle shows an oxide shell (gray) and silicon-rich lamellas (dark gray), which surround a large metallic nucleus (white).

small volume (~15 percent) or may indicate that rapid cooling left the silicate phase in an amorphous state.

Three of the four Group III particles were ellipsoidal and had a brownish, dull, pitted surface. The fourth appeared externally to be similar to spherules from Groups I and II. The particles in Group III consist of poor-

ly crystalline magnetite and goethite, and the polished sections reveal no distinctive internal structure. All contained major iron with trace to minor amounts of Ni, Si, Mn, Mg, Al, Ti, Cr, and Ca. The Group III particles were found in only two of the 21 nodules investigated.

The primary criterion for identifying

cosmic spherules has been the presence of meteoritic quantities of nickel (6), although the absence of nickel does not preclude a cosmic origin (7). Most spherules with a high nickel content have been shown to consist of a metallic core surrounded by an oxide phase (8). Wüstite (FeO), a rare terrestrial mineral, occurs commonly in spherules

Table 1. Summary of petrographic, x-ray diffraction, and electron microprobe analysis. Sample names correspond to oceanographic stations (13). A single dimension in the second column implies that the particle is spherical; two dimensions imply that the particle is elliptical. The precession camera was used with unfiltered Mo radiation. A 57.3-mm Debye-Scherrer powder camera was used with unfiltered Fe radiation: S, spotty pattern; L, line pattern; St, streaky pattern. The polishing technique is described by Finkelman and Duke (14). Iron and nickel analyses were standardized against synthetic nickel-iron alloys. Accuracy is better than ± 2 percent of the amount present. Other elements were determined qualitatively by scaling peaks on spectral scans using a variety of silicate and oxide standards.

Sample and particle No.	Size (μm)	Precession camera results	Powder camera results	Polished section features	Electron microprobe results (percent by weight)					
					Fe	Ni	Co	Si	Mn	Others
Group I particles										
P6604A-001-06 No. 1	130	Single crystals of magnetite* + unidentified phase	Magnetite (S)	Metallic nucleus	25	74	1			
			Wüstite (S)							
			α iron (L)	Oxide shell	70–75	3–4	0.5			
Mero 2P50, No. 1	120	Single crystal of magnetite*	Magnetite (S)	Metallic nucleus	53	48	1			
			Wüstite (S)	Unresolved oxide	65–75	1	tr			
			α iron (L)	phases						
Dodo 113D, No. 1	150	Single crystal of magnetite*	Magnetite (S)	Oxide phase	65–75	1	tr		tr	
Dodo 113D, No. 2	150	Single crystal of magnetite*	Wüstite (S)	Cavity						
			Magnetite (S)	Oxide phase						
			Wüstite (S)	Cavity						
Brunn 95, No. 1	140	Single crystal of magnetite*	Magnetite (S)							
			Wüstite (S)							
			α iron (L)							
Challenger 276, No. 1	120		Magnetite (S)	Metallic nucleus	44	57	2			
			Wüstite (S)	Oxidized nucleus	44.5	14	1			
			Taenite (L)	Dark oxide phase	53.5	1	0.4			
			Maghemite (S)	Light oxide phase	58.5	0.6	0.3			
Challenger 276, No. 5	135		Magnetite (S)	Unresolved oxide	65–75	2.5	0.1			
			Wüstite (S)	phases						
Challenger 276, No. 7	140		Magnetite (S)	Metallic nucleus						
			Wüstite (S)	Oxide shell						
			Taenite (L)							
Vema 15, No. 1	90		Magnetite (S)	Metallic nucleus						
			Wüstite (S)	Oxide shell						
			Taenite (L)							
Albatross 13, No. 1	180		Magnetite (S)							
			Wüstite (S)	Metal (?)						
			α iron (L)							
Group II particles										
Downwind 15, No. 1	140		Magnetite (St)	Unresolved oxide	55	tr		1		Mg(0.1),
			Wüstite (St)	and dark					Al(tr),	
			α iron (L)	lamellas					Ca(tr)	
Downwind 47, No. 1	250 130	Several magnetite crystals with preferred orientation	Magnetite (St)	Oxide phase	65–70	tr				
			Wüstite (St)	Dark lamellas	50			3–9	Mg(1.0),	
			Goethite (L)						Al(tr),	
Albatross 13, No. 2	140		Magnetite (St)	Metallic nucleus	80	20	tr			
			Wüstite (St)	Unresolved oxide	65	tr		1	Mg(0.3),	
			α iron (L)	and dark lamellas					Al(tr),	
Group III particles										
Middle Pacific 126C, No. 1	200 150	Poorly crystalline	Magnetite (L)							
			Goethite (L)							
Middle Pacific 126C, No. 2	170 125	Poorly crystalline	Goethite (L)	Grayish-brown oxide phase	55–67	tr		tr	tr	Mg, Al, Ti, Cr, Ca
			Magnetite (L)							
Albatross 13, No. 7	163 150	Poorly crystalline	Magnetite (L)	Grayish-brown oxide phase	50–70	1		7	tr	Mg, Al, Ti, Cr, Ca
			Goethite (L)							
Albatross 13, No. 8	143 130	Poorly crystalline	Magnetite (L)	Grayish-brown oxide phase	55–65	1	tr	tr	1	Mg, Al, Ti, Ca
			Goethite (L)							
Unclassified particles										
Challenger 285, No. 1	143 130	Poorly crystalline	Goethite (L)	Grayish-brown oxide phase	65			tr		Mg, Al, Ti, Ca, Cr, V
			Magnetite (L)	(nucleus plucked out on polishing)						
Middle Pacific 126C, No. 3	130 100	Poorly crystalline	Magnetite (L)	Gray oxide phase	58–67				0.5	Mg, Al, Ti, Ca, P, V
			Goethite (L)	Dark-gray blebs						
			Grayish-brown oxide nucleus	(Similar analysis for all three phases)						

* $\alpha = 8.40$.

of extraterrestrial origin (9). Wüstite may be produced in industrial processes, but the manganese nodules studied are believed to be several million years old (10), which precludes the possibility of contamination by industrial particles.

On the basis of these criteria, the evidence suggests that both Group I and Group II particles are extraterrestrial in origin. The absence of elements other than Fe, Ni, and Co indicates that Group I particles are apparently ablation products of iron meteorites or of the metallic fraction of stony meteorites. The Si, Mg, Al, and Ca detected in Group II particles suggest that these particles are ablation products of stony meteorites. These elements are among the most common elements in stony meteorites, but they are essentially absent in iron meteorites (11). The presence of a metallic nucleus in the Group II particles is not inconsistent with an origin from stony meteorites, which contain significant quantities of metallic nickel-iron.

The presence of significant amounts of titanium and manganese in Group III particles is highly suggestive of a terrestrial origin (5). The ellipsoidal shape of these particles indicates that they were once molten droplets. The similarity of the chemical analysis to the analysis of magnetic spheroids derived from recent volcanic eruptions (12) and the proximity of these samples to the Hawaiian Islands suggests a volcanic origin.

Two particles have characteristics common to more than one category; they have internal structures similar to those of Groups I and II but chemical compositions similar to Group III particles. It is possible that they are Group I particles that have undergone intense weathering.

ROBERT B. FINKELMAN
U.S. Geological Survey,
Washington, D.C. 20242

References and Notes

1. J. Murray and A. Renard, *Proc. Roy. Soc. Edinburgh Sect. A*, **12** (1884).
2. H. Menard, *Marine Geology of the Pacific* (McGraw-Hill, New York, 1964). The mechanism that prevents the nodules from being buried by the sediment is still unknown.
3. A. Brownlow, W. Hunter, D. Parkin, *Geophys. J.*, **12**, 1 (1966).
4. T. Mutch, *J. Geophys. Res.*, **69**, 4735 (1964).
5. U. Marvin and M. Einaudi, *Geochim. Cosmochim. Acta*, **31**, 1871 (1967).
6. R. Schmidt and K. Keil, *ibid.*, **30**, 471 (1966).
7. A. El Goresy, *Contrib. Mineral. Petrol.*, **17**, 331 (1968).
8. H. Fechtig and K. Uteck, *Ann. N.Y. Acad. Sci.*, **119**, 1 (1964).
9. U. Marvin and M. Einaudi, *Geochim.*

- Cosmochim. Acta*, **31**, 1871 (1967); H. Millard and R. Finkelman, *J. Geophys. Res.*, in press.
10. S. Barnes and J. Dymond, *Nature*, **213**, 1218 (1967).
11. B. Mason, *Meteorites* (Wiley, New York, 1962).
12. F. Wright and P. Hodge, *J. Geophys. Res.*, **70**, 3889 (1965).
13. Coordinates of most stations may be found in J. Mero, *The Mineral Resources of the Sea* (Elsevier, New York, 1965).
14. R. Finkelman and M. Duke, *Amer. Mineral.*, **53**, 1056 (1968).
15. I thank Drs. Michael B. Duke and Daniel Appleman (U.S. Geological Survey), Dr. Frederic Siegel (George Washington University), and Dr. Robin Brett (National Aeronautics and Space Administration) for their valuable assistance.

13 October 1969; revised 1 December 1969

The Ocean: A Natural Source of Carbon Monoxide

Abstract. *The surface waters of the western Atlantic are supersaturated with respect to the partial pressure of carbon monoxide in the atmosphere. Under these conditions, the net transport of carbon monoxide across the air-sea interface must be from the sea into the atmosphere. Thus, the ocean appears to act as a source of carbon monoxide. The ocean may be the largest known natural source of this gas, contributing possibly as much as 5 percent of the amount generated by burning of fuels by man.*

It is generally agreed that the largest single source of carbon monoxide in the atmosphere is the burning of fuel by man, which at the present time is estimated to produce approximately 2×10^{14} g (200 million tons) per year of this toxic pollutant (1). Several natural sources of carbon monoxide have also been reported (2); however, no estimate of output of these sources is available. Despite a continually increasing rate of input into the atmosphere, the background amount of carbon monoxide in the marine atmosphere far removed from sources of pollution appears to be remaining at approximately 0.1 ppm (1, 3). Efficient mechanisms of removal must therefore exist, but the nature of these processes is not clear (2). In order to determine the possible role of the oceans as a sink for this pollutant, we undertook an investigation of the distribution of carbon monoxide between the atmosphere and surface waters. Preliminary results indicated that the surface waters are supersaturated in carbon monoxide with respect to the partial pressure of this gas in the atmosphere (3). Addi-

tional data we now present confirm these findings, and it now appears that rather than acting as a sink the ocean may indeed be the largest natural source of carbon monoxide now known.

During a recent oceanographic cruise in the Atlantic, two 24-hour stations were occupied at which both air and surface water samples were taken at 2-hour intervals. All samples were collected and analyzed within 1 hour of collection by methods previously described (3). The stations were at $13^{\circ}13.9'N$, $59^{\circ}07'W$ (approximately 64 km east of Barbados), and $10^{\circ}38'N$, $60^{\circ}05'W$ (about 112 km east of Trinidad), respectively. At both locations, the prevailing easterly trade winds minimize the possibility of contamination from man-made sources of pollution. The biological characteristics of the water at the two stations, however, differ significantly; the water in the vicinity of the first station is much lower in overall productivity than that at the second station (4).

Two characteristics of the data (Fig. 1) are evident: (i) the relatively constant concentration of CO in the atmosphere at both locations, and (ii) a marked diurnal effect with respect to concentration of CO in the surface waters. The average atmospheric concentrations of 0.14 ppm and 0.09 ppm at stations 1 and 2, respectively, agree with values previously reported for clean marine air of 0.05 ppm (1), and 0.08 ppm (3). They are also in agreement with an average value of 0.09 ppm (5) for Arctic air. The surface water concentrations of CO showed a greater diurnal effect at station 2, which may possibly be related to the high biological productivity of these waters as compared to station 1. The concentrations of dissolved CO between 10^{-4} and 10^{-5} ml/liter agree with values reported for western Atlantic waters (3), and also with unpublished values of from 1 to 3×10^{-5} ml/liter found by us in the vicinity of the Chesapeake Light Tower, some 24 km from the entrance to Chesapeake Bay. The observed decrease in dissolved CO during the late afternoon and early evening hours appears to be accompanied by a slight but significant increase in atmospheric CO. That the correlation is not more clearly evident is likely due to very rapid mixing in the atmosphere, since the wind velocities during all sampling operations were between 10 and 15 knots.

A state of nonequilibrium between